

BBAMEM 75452

## Transport-related modulation of the membrane properties of toad urinary bladder epithelium

Simon A. Lewis<sup>1</sup>, Chris Clausen<sup>2</sup> and Nancy K. Wills<sup>1</sup>

<sup>1</sup> Departments of Physiology and Biophysics, University of Texas, Medical Branch, Galveston TX, (U.S.A.)  
and <sup>2</sup> State University of New York, Stony Brook, NY (U.S.A.)

(Received 21 June 1991)

Key words: Impedance analysis; Sodium ion transport; Anion; Amiloride; (Toad urinary bladder)

Impedance analysis and transepithelial electrical measurements were used to assess the effects of the apical membrane Na<sup>+</sup> channel blocker amiloride and anion replacement on the apical and basolateral membrane conductances and areas of the toad urinary bladder (*Bufo marinus*). Mucosal amiloride addition decreased both apical and basolateral membrane conductances ( $G_a$  and  $G_{bl}$ , respectively) with no change in membrane capacitances ( $C_a$  and  $C_{bl}$ ). Consequently, the specific conductances of these membranes decreased without significant changes in membrane area. Following amiloride removal, an increase was obtained in the steady-state rate of sodium transport compared to values before amiloride addition. This increase was independent of the initial transport rate, suggesting activation of a quiescent pool of apical sodium channels. Chloride replacement by acetate or gluconate had no significant effects on apical or basolateral membrane capacitances. The effects of these replacements on membrane conductances depended on the anion species. Gluconate (which induces cell shrinkage) decreased both membrane conductances. In contrast, acetate (which induces cell swelling) increased  $G_a$  and had no effect on  $G_{bl}$ . The increase in the apical membrane conductance was due to an increase in the amiloride-sensitive Na<sup>+</sup> conductance of this membrane. In summary, mucosal amiloride addition or chloride replacements led to changes in membrane conductances without significant effects on net membrane areas.

### Introduction

The toad urinary bladder (*Bufo marinus*) has been used as a model system to study the mechanisms involved in the regulation of sodium transport across tight epithelia [1]. Increasing evidence suggests that alterations in the rate of Na<sup>+</sup> entry across the apical membrane (e.g. using the Na<sup>+</sup> channel blocker amiloride) modifies the permeability of the basolateral membrane to K<sup>+</sup> and conversely, modification of basolateral membrane K<sup>+</sup> permeability or Na-K pump activity modifies apical membrane Na<sup>+</sup> permeability. This process has been referred to as crosstalk or homocellular regulation between the apical and basolateral membranes [2,3].

In addition to this regulation, several studies have shown that replacement of mucosal or serosal chloride

with other anions can also affect transepithelial sodium transport [4]. Lewis et al. [5] determined that replacement of bathing solution chloride by gluconate decreased transepithelial short-circuit current ( $I_{sc}$ ) and shifted amiloride binding kinetics. This decrease in  $I_{sc}$  by serosal gluconate was due to a decrease in the basolateral membrane K<sup>+</sup> permeability. In contrast, replacement of bathing solution chloride with acetate, stimulated transepithelial sodium transport without any apparent change in the basolateral membrane K<sup>+</sup> permeability. These alterations in transport by anion replacements were also accompanied by alterations in cell volume: gluconate produced cell shrinkage whereas, acetate, in contrast, resulted (in some instances) in cell swelling [5].

The objectives of this study were two-fold. First was to develop a morphologically based electrical equivalent circuit model of the toad urinary bladder using impedance analysis. Such a model will yield estimates of both the individual membrane conductances and the individual membrane areas, measured as capacitance. Second was to utilize this equivalent circuit, in con-

Correspondence: S.A. Lewis, Department of Physiology and Biophysics, University of Texas Medical Branch, Galveston, TX 77550, U.S.A.

junction with well established electrophysiological techniques, to investigate the effects of altered rates of transepithelial  $\text{Na}^+$  transport on the membrane conductances and membrane areas of the toad urinary bladder.

## Methods

Toads (*Bufo marinus*) obtained from the Dominican Republic (National Reagents, Inc.) were killed using the double pith method. Hemi-bladders were removed and then mounted in modified Ussing chambers [6] designed to eliminate edge damage and giving a nominal surface area of  $2 \text{ cm}^2$ . The serosal side was supported against a nylon mesh by a slight excess of mucosal solution. Both mucosal and serosal solutions were bubbled with air and stirred by magnetic spin bars in the bottom of each chamber. All experiments were carried out at room temperature ( $20\text{--}22^\circ\text{C}$ ).

## Solutions

All solutions were prepared from analytical grade reagents. Sodium chloride Ringer's solution contained in mM: 112 NaCl, 3.5 KCl, 1.0  $\text{CaCl}_2$ , 1.0  $\text{MgSO}_4$ , 10 glucose, and was buffered at pH 7.8 with 2 mM  $\text{Na}_2\text{HPO}_4$ . Chloride-free Ringer's solutions were prepared from either the gluconate or acetate salts of  $\text{Na}^+$ ,  $\text{K}^+$ , and  $\text{Ca}^{2+}$  at concentrations equal to that of the chloride salts. The remaining salts and glucose were the same as in the chloride Ringer's solution. Amiloride (a gift from Merck, Sharp, and Dohme) was prepared as a stock solution in distilled water. Microliter quantities were added to bring the mucosal concentration to  $10^{-4} \text{ M}$ .

## Electrical measurements

All measurements were made under open circuit conditions. Spontaneous transepithelial voltage ( $V_T$ ) was monitored using a pair of 3 M KCl agar bridges connected to Ag-AgCl wires, led to the differential inputs of a PARC 113A low noise amplifier. To measure resistance, a square current pulse 200 ms in duration and large enough to cause a 20 mV deflection in  $V_T$  was passed across the epithelium.

The transepithelial resistance ( $R_T$ ) was calculated from the deflection in  $V_T$  and the current pulse amplitude using Ohm's law. Short-circuit current was similarly calculated from  $V_T$  and  $R_T$ . Junctional resistance ( $R_j$ ) and cellular electromotive force ( $E_c$ ) were calculated using the method of Yonath and Civan [7] as adapted by Wills et al. [8] (see also Ref. 5). Briefly, this method involves amiloride addition to the mucosal bathing solution.  $R_T$  and  $V_T$  are measured before and during amiloride action. A plot of  $V_T$  versus  $R_T$  yields a linear double-intercept plot where the  $V_T$  intercept is equivalent to  $E_c$  and the  $R_T$  intercept is equal to  $R_j$ .

## Transepithelial impedance analysis

Transepithelial impedance was measured using the methods described in Clausen, Reinach and Marcus [9]. The method includes the use of a wide-band pseudo-random binary noise signal which is generated digitally and converted to a constant current signal of 1.4 and  $14 \mu\text{A}/\text{cm}^2$  (peak-to-peak) at low and high bandwidths, respectively. Two signal bandwidths were employed (2.2 to 860 Hz and 22 Hz to 8.6 kHz) to provide good resolution at high and low frequencies. The transepithelial voltage produced in response to this signal was measured using a low noise amplifier and filtered through a 120 dB/octave low-pass anti-aliasing filter (Unigon, Inc.). Digitization of the current and voltage signals and data acquisition were controlled by a PDP 11-34 computer (Digital Equip. Corp.) with a 12 bit A-D converter. Signals were also averaged by the computer to increase the signal-to-noise ratio. Data acquisition time was less than 5 s per run.

Transepithelial impedance was calculated by dividing the cross-spectral density of the voltage and current by the power spectral density of the applied current. This resulted in 400 data points linearly spaced for the low frequency bandwidth and another 400 for the high frequency bandwidth. These 800 points were then merged and reduced to 100 data points, logarithmically spaced in frequency from 2.2 Hz to 8.6 kHz. Each data point consisted of two numbers: a phase angle and a magnitude.

The data were then fitted by a morphologically-based equivalent-circuit model using a non-linear least-squares curve fitting algorithm (for details of this computer-generated curve fitting procedure, see Refs. 10 and 11). In the equivalent circuit model, resistors were used to represent membrane ionic conductance and capacitors were used to represent membrane capacitance which is proportional to membrane area ( $1 \mu\text{F} \equiv 1 \text{ cm}^2$  membrane area [12]). Two criteria were used to evaluate the quality of the fits to the data: (1) the Hamilton  $R$ -factor and (2) parameter standard deviations (computed assuming linearized model parameters [10]). A large value for either criteria was defined as a poor fit of the data. Specifically, fits yielding  $R$ -factor values of more than 3.5% or standard deviations of more than 10% of the fitted parameter value were defined as poor fits and the data were excluded from further analysis. For further details of the analysis procedure see Wills and Clausen [11].

## Results

In this section, we will first evaluate four morphologically-based equivalent circuit models of the toad urinary bladder. We then select the equivalent circuit model that best describes the impedance properties of this epithelium. Next, we describe the effects of mu-

cosal amiloride on membrane impedance properties, (i.e. membrane conductances and capacitances where capacitance is an index of membrane area). Lastly, the effects of chloride substitution by gluconate or acetate on membrane properties and transepithelial  $\text{Na}^+$  transport are reported.

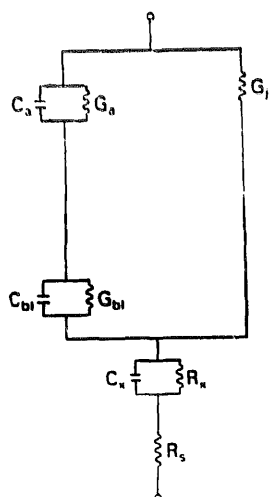
### Evaluation of equivalent circuit models

**Morphological considerations.** The epithelial cell layer of the toad urinary bladder is composed of three distinct cell types: (1) the granular cells which are responsible for sodium and water transport and represent about 75% of the total number of cells, (2) the mitochondria-rich cells and (3) mucous secreting goblet

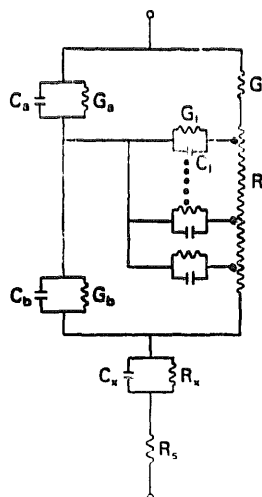
cells. The latter two cell types each account for approximately 12.5% of the total cell number. In addition to the epithelial cell layer, the bladder is also composed of basal cell layers, smooth muscle bundles and a peritoneal epithelium (for a complete description of toad bladder morphology [13]).

**Description of circuit elements.** In Figs. 1A-D the morphological features of the toad bladder are represented as four equivalent circuits composed of resistors and capacitors. Note that the equivalent circuit models shown here are the most simple models and combine all three types of epithelial cells into a single cell which represents the mean conductance and capacitance properties of the total epithelial cell population. In Fig.

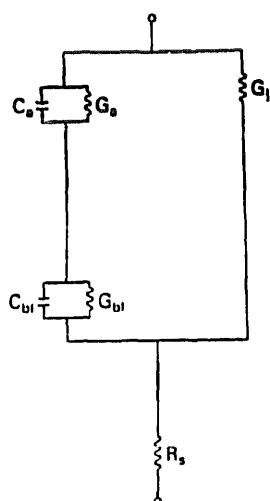
A) LUMPED 2-CELL MODEL



B) DISTRIBUTED 2-CELL MODEL



C) LUMPED 1-CELL MODEL



D) DISTRIBUTED 1-CELL MODEL

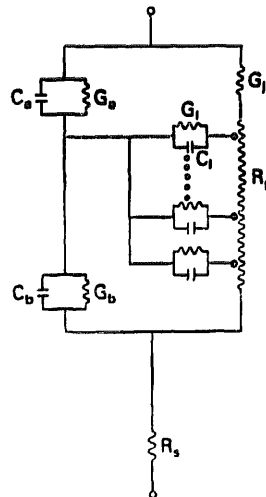


Fig. 1. Equivalent circuit models used to represent transepithelial impedance. (A) Lumped 2-cell layer model.  $G_a$  and  $C_a$  are apical membrane conductance and capacitance,  $G_{bl}$  and  $C_{bl}$  are basolateral membrane conductance and capacitance,  $G_l$  is tight junctional conductance.  $R_s$  is solution series resistance and  $R_x$  and  $C_x$  are the net resistance and capacitance of an extraepithelial cell layer. (B) Distributed 2-cell layer model. In this case, the basal membrane impedance is treated as a single entity ( $G_b$  and  $C_b$ ) while the lateral membrane impedance ( $C_l$  and  $G_l$ ) is distributed along the lateral intercellular space resistance (represented as  $R_p$ ). (C) and (D) Simplified lumped (C) and distributed (D) models.

The extra-epithelial layer  $R_x C_x$  has been removed from both models.

TABLE I

Estimates of membrane impedance parameters by different equivalent circuit models

Model	$G_j$ ( $\mu\text{S}/\text{cm}^2$ )	$G_a$ ( $\mu\text{S}/\text{cm}^2$ )	$C_a$ ( $\mu\text{F}/\text{cm}^2$ )	$G_{bl}$ ( $\text{mS}/\text{cm}^2$ )	$C_{bl}$ ( $\mu\text{F}/\text{cm}^2$ )	$R_p$ ( $\Omega \text{ cm}^2$ )	$R_x$ ( $\Omega \text{ cm}^2$ )	$C_x$ ( $\mu\text{F}/\text{cm}^2$ )	$R_s$ ( $\Omega \text{ cm}^2$ )	$R$ -factor (%)
A Distributed										
2-cell layer	82 $\pm$ 12	62 $\pm$ 17	0.9 $\pm$ 0.05	2.0 $\pm$ 0.3	4.1 $\pm$ 0.5	50 $\pm$ 26	83 $\pm$ 21	4.1 $\pm$ 0.5	95 $\pm$ 5	0.6 $\pm$ 0.04
B Lumped										
2-cell layer	82 $\pm$ 12	62 $\pm$ 17	0.9 $\pm$ 0.04	2.4 $\pm$ 0.3	3.6 $\pm$ 0.4	—	62 $\pm$ 14	3.4 $\pm$ 0.5	101 $\pm$ 4	0.7 $\pm$ 0.8
C Distributed										
1-cell layer	82 $\pm$ 12	62 $\pm$ 16	0.9 $\pm$ 0.04	4.1 $\pm$ 0.5 *	3.7 $\pm$ 0.4	220 $\pm$ 141	—	—	88 $\pm$ 5 *	1.2 $\pm$ 18 *

\*  $P < 0.05$  compared to the distributed 2-cell layer model; paired  $t$ -test.

1A, the apical membrane is modeled as a parallel resistor and capacitor ( $R_a$  and  $C_a$ , respectively) arranged in series with the basolateral membrane which, in turn, is modeled as a parallel combination of resistor and capacitor ( $R_{bl}$  and  $C_{bl}$  respectively). This cellular pathway is shunted by the tight junctional resistance ( $R_j$ ) and the epithelial circuit is in series with the solution resistance,  $R_s$ . In addition, another extra-epithelial parallel resistor/capacitor combination ( $R_x$  and  $C_x$ ) is placed in series with the epithelial impedance and solution resistance.  $R_x C_x$  represents the combined RC properties of many cell types, in this case, the mean properties of the extra-epithelial cell layers (i.e., basal cells, muscle cells, etc.). The circuit shown in Fig. 1B takes into account an additional morphological feature of the epithelium, the lateral intercellular spaces (LIS), represented as the resistor,  $R_p$ . This so-called epithelial distributed model [14] differs from the 'lumped' model (shown in Fig. 1A) in that the lateral membrane impedance properties are distributed along the length of the lateral space, i.e., the lateral membrane impedance and lateral space resistance are comparable at high frequencies.

Use of either of these so-called '2-cell layer' models [9] given in Figs. 1(A and B) resulted in good fits to the data (see Table I: lines A and B). Moreover, the different models gave nearly identical estimates of membrane parameters. A small improvement of fit was obtained using the distributed model (mean  $R$ -factor =  $0.58 \pm 0.04\%$ ) compared to the lumped model ( $R$ -factor =  $0.73 \pm 0.08$ ;  $n = 9$  bladders). In 4 out of the 9 tissues, the best fit values for the lateral intercellular space resistance ( $R_p$ ) was less than  $0.1 \Omega$ . In these experiments, the best-fit values for other circuit parameters estimated by the two models were identical. This is expected since in the absence of a significant lateral space resistance, the distributed model (Fig. 1B) simplifies to the lumped model (Fig. 1A).

To assess whether the addition of the extra-epithelial cell layer was necessary to adequately fit the data, we next eliminated this RC component and refitted the data using the more simple '1-cell layer' lumped and distributed models given in Figs. 1(C and D). In 8

of the 9 bladders, the lumped 1-cell layer model could not fit the data according to the criteria for adequacy of fit. Although the distributed 1-cell layer model was able to meet the fit criteria, predominate regions of misfit were noted for the phase data over the entire frequency range. The misfit was independent of the experimental condition.

A comparison of the model fits and data for the 1-cell layer and 2-cell layer distributed models is given in Figs. 2(A and B). Although the differences between the two model fits appear to be slight, Fig. 2C illustrates the residual differences between the model fits and the data. Note the systematic variations in the results of the simplified model which are eliminated by use of the extra-epithelial layer model.

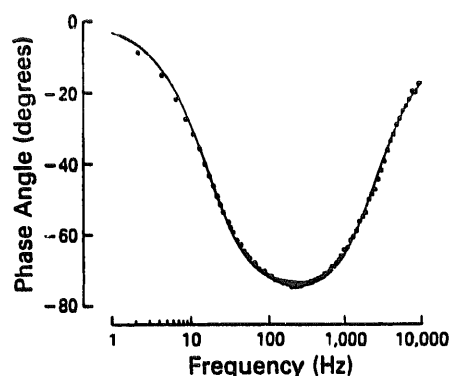
Further comparison of these two models can be made by inspection of Table I which summarizes parameter values derived from the 1-cell layer distributed model (line C) and from the 2-cell layer distributed model (line A). Use of the 2-cell layer model led to significantly lower estimates of the basolateral membrane conductance ( $G_{bl}$ ) and a small but significantly larger estimate of the series (solution) resistance. The lower  $R$ -factor measurement for this model was expected since the addition of extra parameters will invariably result in a better fit to the data. To verify that the quality of the measured impedance warrants the addition of the extraepithelial circuit parameters, an  $R$ -ratio test (a modified  $F$ -test, [15]) was performed comparing the results of the two distributed models. In all cases, the two cell model resulted in a highly significant ( $P < 0.001$ ) reduction in the  $R$ -factor, thereby indicating that the reduction in the final sum-square error was not simply fortuitous.

Because of the superior fits by the 2-cell layer distributed model and the general similarity of membrane parameter estimates for the 1 cell-layer and 2-cell layer models, we present below results only for the 2-cell layer distributed model, i.e., the model which contains an extra-epithelial barrier defined as the series element,  $R_x C_x$ . In the absence of a significant lateral space resistance, this model simplifies to the lumped 2-cell layer model (see above).

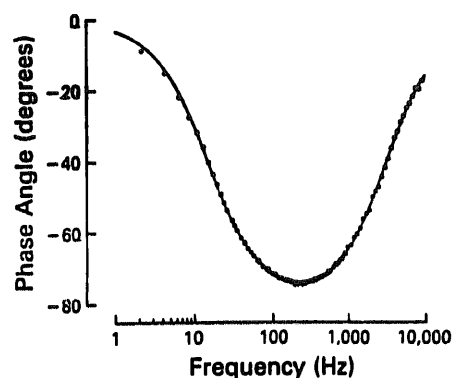
### Transepithelial effects of amiloride and estimate of $R_j$

In normal NaCl Ringer's solutions, the toad urinary bladder had a spontaneous transepithelial potential ( $V_T$ ) of  $-35 \pm 3$  mV ( $n = 24$ , 9 bladders), a transepithelial resistance ( $R_T$ ) of  $8.8 \pm 2.6$  k $\Omega$  cm<sup>2</sup>, and a calculated short-circuit current ( $I_{sc}$ ) of  $4.2 \pm 1.9$   $\mu$ A/cm<sup>2</sup>. Addition of  $10^{-4}$  M amiloride to the mucosal chamber decreased  $V_T$  to  $-10 \pm 1$  mV and  $I_{sc}$  to  $0.7 \pm 0.3$   $\mu$ A/cm<sup>2</sup>.  $R_T$  was increased to  $13 \pm 5$  k $\Omega$  cm<sup>2</sup>. An interesting feature, previously reported by Garty and Edelman [16], was that the amiloride-sensitive current was larger ( $62 \pm 20\%$ ;  $n = 9$ ) after a previous 10-min incubation with amiloride compared to the

#### A. DISTRIBUTED



#### B. DISTRIBUTED 2-CELL



#### C. RESIDUALS

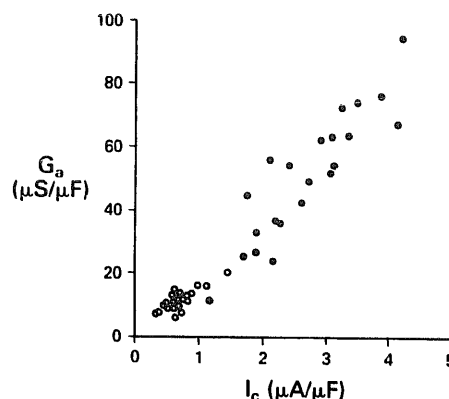
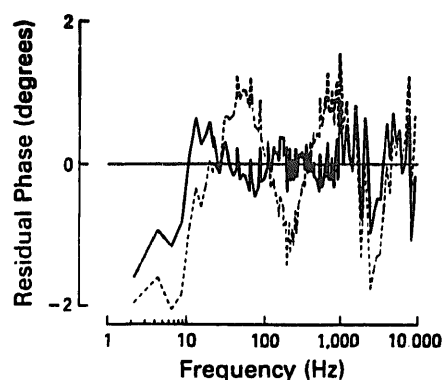


Fig. 3. A plot of the apical membrane conductance and cellular current (apical membrane current). The closed circles are currents measured in control (NaCl) Ringers, the open circles are after adding  $10^{-4}$  M amiloride to the mucosal solution. A curvilinear behavior between current and conductance is expected since for open circuit conditions, as  $G_a$  decreases the net electrochemical gradient favoring Na entry increases, i.e., cell membrane potential referenced to the mucosal solution becomes more negative.

absence of previous amiloride exposure. The amiloride-insensitive current was unchanged.

(i)  $R_j$  estimate. As previously described by Clausen et al. [14], to calculate membrane resistance and capacitance values from impedance data, it is necessary to independently measure at least one circuit parameter. Since microelectrodes were not employed in this study, we estimated tight junctional resistance ( $R_j$ ). This value and the cellular electromotive force ( $E_C$ ) were calculated by measuring the response of  $V_T$  and  $R_T$  to a saturating dose of amiloride as summarized in Methods (see also Refs. 5 and 8). The circuit parameters for control and amiloride inhibition of transport are summarized in Table II, together with the estimates for tight junctional conductance ( $1/R_j$  or  $G_j$ ) and  $E_C$ . In

Fig. 2. (A) Representative results showing a Bode plot of impedance phase angle for a toad urinary bladder bathed in  $\text{Cl}^-$  Ringer's solution. Symbols are measured data and solid lines are the fit by a simplified distributed model (for description, see text). Using a measured  $G_j = 82.5$   $\mu$ S (for 2 cm<sup>2</sup> of tissue), the results of the fit were as follows:  $G_a = 102$   $\mu$ S,  $C_a = 1.69$   $\mu$ F,  $G_{bl} = 8.4$  mS,  $C_{bl} = 6.3$   $\mu$ F,  $R_p = 19.8$   $\Omega$ ,  $R_s = 40.9$   $\Omega$ ,  $R$ -factor = 1.01%. (B) The same data fit by the distributed two cell layer model (see Fig. 1b) using the same  $G_j$  as above. A significant improvement in fit was obtained. The results of the fit were as follows:  $G_a = 101$   $\mu$ S,  $C_a = 1.8$   $\mu$ F,  $G_{bl} = 4.27$  mS,  $C_{bl} = 8.7$   $\mu$ F,  $R_p = 9.1$   $\Omega$ ,  $R_s = 43.1$   $\Omega$ ,  $R_x = 31$   $\Omega$ ,  $C_x = 9.1$   $\mu$ F,  $R$ -factor = 0.52%. (C) Phase angle residuals (differences between the data and model) derived from fits by the simplified model (dashed line) and two cell layer model (solid line) to the same data. The simplified model resulted in systematic deviations which appear as 'sinusoidal-like' variations in the residual plot. These deviations were nearly eliminated by the 2-cell layer model, resulting in a 'noise-like' plot typical of small measurement errors. The residuals at the four lowest frequencies (< 10 Hz) most likely reflect effects caused by ion accumulation and/or depletion in small restricted spaces; these effects are not accounted for in the models (see Discussion).

TABLE II

Effect of amiloride on impedance-derived parameters ( $n = 24$ )

	$E_c$ (mV)	$G_j$ ( $\mu S/cm^2$ )	$G_a$ ( $\mu S/cm^2$ )	$C_a$ ( $\mu F/cm^2$ )	$G_{bl}$ ( $mS/cm^2$ )	$C_{bl}$ ( $\mu F/cm^2$ )	$R_p$ ( $\Omega cm^2$ )	$R_x$ ( $\Omega cm^2$ )	$C_x$ ( $\mu F/cm^2$ )	$R_s$ ( $\Omega cm^2$ )
NaCl	$117 \pm 8$	$83 \pm 9$	$46.7 \pm 20.5$	$0.9 \pm 0.18$	$1.8 \pm 0.65$	$4.1 \pm 1.35$	$104 \pm 34$	$94 \pm 16$	$3.8 \pm 2.5$	$96 \pm 2.9$
Amiloride			$11.2 \pm 4.4^*$	$0.9 \pm 0.16$	$1.3 \pm 0.75^*$	$4.2 \pm 1.35$	$100 \pm 32$	$108 \pm 16$	$3.6 \pm 0.2$	$97 \pm 2.8$

\*  $P < 0.001$ .

the following sections, we will consider the properties of each membrane along with the effects of amiloride on their impedance.

(ii) *Apical membrane properties.* Mucosal addition of amiloride decreased apical membrane resistance without altering the capacitance of this membrane. The decrease in conductance ( $\approx 72\%$ ) was proportional to the decrease in  $I_{sc}$  of  $\approx 78\%$ . Note that under the open circuit conditions used in the present study,  $I_{sc}$  is an overestimate of the cellular current flow ( $I_c$ , the current which moves across both the apical and basolateral membrane). This current flow ( $I_c$ ) can be calculated as the product of  $V_T$  and  $G_j$  [17]. Fig. 3 shows the relationship between apical membrane current and conductance before and after amiloride addition.

As stated above, the amiloride-sensitive current was increased by  $\approx 62\%$  following incubation in amiloride. This increase in current was accounted for by a  $42 \pm 17\%$  ( $P < 0.05$ ;  $n = 9$ ) increase in apical membrane sodium conductance without an significant change in membrane capacitance ( $1.7 \pm 1.6\%$  n.s.;  $n = 9$ ). Therefore, the increase in sodium conductance induced after amiloride incubation was not accompanied by an appreciable increase in membrane area. Fig. 4 shows that this increase is not correlated with the initial amiloride-sensitive  $Na^+$  transport rate. This will be addressed in more detail in the discussion.

(iii) *Basolateral membrane impedance.* The basolateral membrane conductance (sum of the conductance of all three cell types) was on average 39-times greater

than the apical membrane conductance. Amiloride resulted in a  $28 \pm 6\%$  decrease in basolateral membrane conductance with no significant change in basolateral membrane capacitance. In contrast to the apical membrane conductance, there was no correlation between cell current and basolateral membrane conductance. This finding suggests that a predominant and variable portion of the basolateral membrane conductance is not associated with transepithelial sodium transport. These findings of a low amiloride sensitive apical membrane conductance are consistent with the relatively low  $I_{sc}$  value ( $4 \mu A/cm^2$ ) in the present study compared to previous studies of toad bladder, as an example an  $I_{sc}$  of  $8 \mu A/cm^2$  [5].

(iv) *Other circuit parameters.* Of the 24 paired control and amiloride impedance runs (from 9 bladders), 13 pairs were best fitted by the distributed two-layer model, whereas the remainder were adequately described by the lumped two-layer model. Fig. 5 shows a plot of apical membrane capacitance (an index of tissue stretch) as a function of  $R_p$ , the LIS resistance. Highly stretched preparations had negligible values for  $R_p$ , while less stretched preparations had high  $R_p$  values.

Neither the solution series resistance ( $R_s$ ) nor the extra-epithelial resistor-capacitor network ( $R_x C_x$ ) were significantly affected by amiloride addition. Free solution resistance was independent of the apical membrane area as measured by apical membrane capacitance. However, as shown in Fig. 6A, there was an

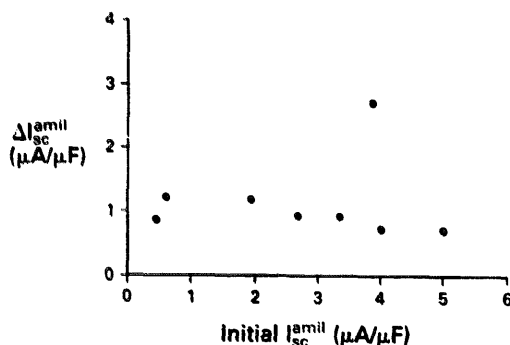


Fig. 4. The magnitude of the amiloride sensitive current increases after a 10-min incubation in  $10^{-4}$  M mucosal amiloride. The absolute increase ( $\Delta I_{sc}$ ) is not correlated with the control (pre-amiloride) amiloride sensitive short circuit current. This suggests that amiloride is activating a population of quiescent channels.

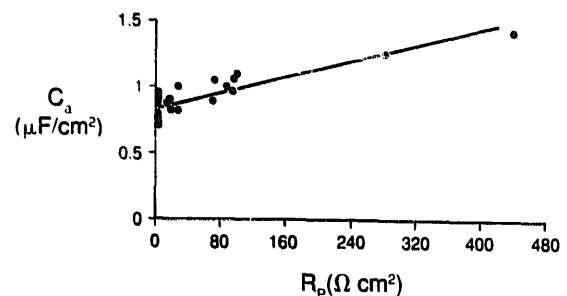


Fig. 5. The relationship between the apical membrane capacitance ( $C_a$ ) and the resistance of the lateral intracellular space ( $R_p$ ). This plot illustrates that there is a direct relationship between surface area and  $R_p$ . Highly stretched preparations (low  $C_a$ ) might have a short LIS path length and dilated spaces, resulting in a low  $R_p$  value, while less stretched preparations will have long path lengths and collapsed spaces.

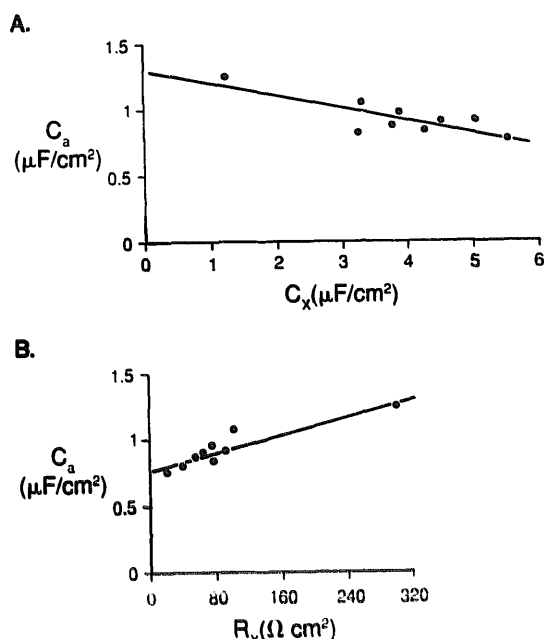


Fig. 6. (A) The correlation between apical surface area and the extrapathelial capacitance ( $C_x$ ). See discussion for possible morphological basis of  $C_x$ . (B) A direct correlation exists between apical surface area and extrapathelial resistance ( $R_x$ ). The lower the apical surface area (more stretched epithelium) the smaller is this resistance. See Discussion for possible morphological basis of  $R_x$ .

inverse correlation between  $C_a$  and  $C_x$  and a direct correlation between apical capacitance and  $R_x$  (see Fig. 6B).

### The effects of anions on membrane properties

#### Gluconate

As previously reported by Lewis et al. [5], the symmetrical replacement of chloride by gluconate caused a significant decrease in  $V_T$  and  $I_{sc}$  from  $-45 \pm 9$  to  $-32 \pm 8$  mV and from  $7.5 \pm 5.1 \mu\text{A}/\text{cm}^2$  to  $1.6 \pm 1.1 \mu\text{A}/\text{cm}^2$ .  $R_T$  increased from  $11.2 \pm 5.8$  to  $20.2 \pm k\Omega \text{ cm}^2$  ( $n = 9$ ). The addition of amiloride to the mucosal solution caused a further decrease in  $V_T$  and  $I_{sc}$  to  $-10 \pm 1$  mV and  $0.5 \pm 0.2 \mu\text{A}/\text{cm}^2$ , respectively, and a further increase in  $R_T$  to  $22.2 \pm 9.2 k\Omega \text{ cm}^2$  ( $n = 9$ ).

The decrease in  $I_{sc}$  is caused by a decrease in the apical membrane sodium permeability and a decrease in the net electrochemical gradient across this membrane caused indirectly by a decrease in the basolateral membrane electromotive force. The increase in  $R_T$  is due both to the decrease in  $G_a$  and a decrease in the paracellular conductance due to the poor permeability of this pathway to gluconate.

The junctional resistance ( $R_j$ ) and cellular electromotive force ( $E_c$ ) were assessed using amiloride in chloride and gluconate Ringer's solutions. The results are summarized in Table III along with the impedance results for these conditions. As reported by Lewis et al. [5], gluconate caused a decrease in the cellular e.m.f. from 123 mV to 80 mV and decreased paracellular conductance from  $74 \mu\text{S}/\text{cm}^2$  to  $46 \mu\text{S}/\text{cm}^2$ . The impedance parameters are discussed below.

(i) *Apical membrane impedance.* The apical membrane conductance was significantly decreased by the symmetrical replacement of chloride by gluconate, but apical membrane capacitance was unchanged. Mucosal addition of amiloride also did not change  $C_a$  under these conditions. However, amiloride decreased the apical membrane conductance to a value that was not statistically different from that of tissues bathed in chloride Ringer's solutions (i.e., the amiloride-insensitive conductance was  $9.5 \pm 1.3 \mu\text{S}/\text{cm}^2$ ).

(ii) *Basolateral membrane impedance.* Basolateral membrane capacitance was not altered by replacing chloride with gluconate, nor by the subsequent addition of amiloride. In contrast, the basolateral membrane conductance decreased by 47% when gluconate replaced chloride. Subsequent mucosal amiloride addition did not significantly decrease  $G_{bl}$ .

(iii) *Other parameters.* Of the 6 paired bladders, 3 required the use of a distributed model when bathed in chloride Ringer's solutions. After replacement of chloride by gluconate, all 6 bladders required the distributed model.  $R_s$  was increased by 80% and  $R_p$  was increased by 31%. These increases are expected since the resistivity of gluconate solutions is greater than that of chloride solutions. Amiloride did not significantly alter either parameter under these conditions.

TABLE III

The effect of symmetrical replacement of  $\text{Cl}^-$  with gluconate on impedance-derived parameters

	$E_c$ (mV)	$G_j$ ( $\mu\text{S}/\text{cm}^2$ )	$G_a$ ( $\mu\text{S}/\text{cm}^2$ )	$C_a$ ( $\mu\text{F}/\text{cm}^2$ )	$G_{bl}$ ( $\mu\text{S}/\text{cm}^2$ )	$C_{bl}$ ( $\mu\text{F}/\text{cm}^2$ )	$R_p$ ( $\Omega \text{ cm}^2$ )	$R_s$ ( $\Omega \text{ cm}^2$ )	$c_x$ ( $\mu\text{F}/\text{cm}^2$ )	$R_s$ ( $\Omega \text{ cm}^2$ )
NaCl	$124 \pm 8.7$	$74 \pm 19$	$42 \pm 20$	$0.93 \pm 0.21$	$1.8 \pm 0.37$	$4.1 \pm 1.0$	$150 \pm 130$	$108 \pm 48$	$3.6 \pm 0.5$	$100 \pm 4.6$
Na gluconate ( $n = 6$ )	$85 \pm 10^*$	$38 \pm 6^*$	$21 \pm 10^*$	$0.92 \pm 0.20$	$0.9 \pm 0.33^*$	$4.2 \pm 0.9$	$220 \pm 110$	$230 \pm 110^*$	$3.9 \pm 0.5$	$181 \pm 5.4^*$
Na gluconate + amiloride ( $n = 9$ )	$80 \pm 8.6$	$45 \pm 6$	$20 \pm 8$ $7.3 \pm 3.5^*$	$0.9 \pm 0.17$ $0.9 \pm 0.17$	$1.0 \pm 0.46$ $0.85 \pm 0.55$	$4.0 \pm 1$ $5.0 \pm 2.4$	$204 \pm 74$ $250 \pm 86$	$202 \pm 80$ $262 \pm 74$	$4.4 \pm 0.5$ $4.5 \pm 0.8$	$174 \pm 7$ $174 \pm 7$

\*  $P < 0.05$ .

TABLE IV

The effect of symmetrical replacement of  $\text{Cl}^-$  with acetate on impedance-derived parameters

	$E_c$ (mV)	$G_j$ ( $\mu\text{S}/\text{cm}^2$ )	$G_a$ ( $\mu\text{S}/\text{cm}^2$ )	$C_a$ ( $\mu\text{F}/\text{cm}^2$ )	$G_{bl}$ ( $\mu\text{F}/\text{cm}^2$ )	$C_{bl}$ ( $\Omega\text{ cm}^2$ )	$R_p$ ( $\Omega\text{ cm}^2$ )	$R_x$ ( $\mu\text{F}/\text{cm}^2$ )	$C_x$ ( $\Omega\text{ cm}^2$ )	$R_s$
NaCl	113 ± 9	91 ± 11	35.6 ± 9.2	0.98 ± 0.2	1.61 ± 0.5	4.1 ± 1.5	70 ± 33	126 ± 44	4.0 ± 0.5	91 ± 4
Na acetate ( $n = 6$ )	100 ± 4 *	66 ± 7 *	42 ± 11 *	1.05 ± 0.2	1.37 ± 1.7	3.9 ± 0.17	144 ± 60 *	150 ± 24 *	3.5 ± 0.4	135 ± 7 *
Na acetate + Amiloride ( $n = 6$ )	100 ± 4	66 ± 7	41 ± 11 12 ± 2.6 *	1.05 ± 0.2 1.1 ± 0.3	1.45 ± 0.6 0.75 ± 0.35 *	3.8 ± 1.9 4.7 ± 2.2	147 ± 57 212 ± 90	149 ± 24 250 ± 60	3.5 ± 0.4 3.5 ± 0.4	136 ± 7 139 ± 7

\*  $P < 0.05$ .

An increase of 98% was measured for  $R_x$  after gluconate replacement of chloride, while  $C_x$  was unchanged. Subsequent amiloride addition did not result in a significant change in either  $R_x$  or in  $C_x$ .

#### Acetate

The symmetrical replacement of chloride with acetate resulted in a significant increase in  $V_T$  (from  $-28 \pm 6$  to  $-37 \pm 5$  mV,  $n = 6$ ),  $I_{sc}$  (from  $3.1 \pm 1.2$  to  $3.7 \pm 1.2$   $\mu\text{A}/\text{cm}^2$ ), and  $R_T$  ( $8.6 \pm 1.8$  to  $10.0 \pm 1.6$   $\text{k}\Omega\text{ cm}^2$ ). Similar changes in these values were previously reported by Lewis et al. [5]. Addition of mucosal amiloride to acetate solutions led to a significant decrease in  $V_T$  (from  $-34 \pm 5$  to  $-10 \pm 2$  mV,  $n = 6$ ) and  $I_{sc}$  (from  $3.6 \pm 1.1$  to  $0.7 \pm 0.3$   $\mu\text{A}/\text{cm}^2$ ).  $R_T$  increased from  $10.0 \pm 1.4$  to  $14.0 \pm 3.4$   $\text{k}\Omega\text{ cm}^2$ . Both the junctional conductance and cellular electromotive force, calculated from the amiloride response, showed significant decreases (see Table IV). These observations are in agreement with previous results [5]. The impedance parameters for this condition are also contained in Table IV and are discussed below.

(i) *Apical and basolateral membrane impedances.* In contrast to the effects of gluconate, the apical membrane conductance was increased significantly when chloride was replaced by acetate. As in the case of gluconate, apical membrane capacitance was unchanged. Addition of amiloride to the mucosal solution also did not alter  $C_a$ , but reduced  $G_a$  to a value not different than the amiloride-insensitive apical membrane conductance when bathed in solutions containing chloride. Unlike the effects of gluconate, there was no change in  $G_{bl}$  when acetate replaced chloride. The subsequent addition of amiloride significantly decreased  $G_{bl}$  with no change in  $C_{bl}$ , similar to the effects of amiloride in chloride-containing solutions.

(ii) *Other parameters.* In 6 paired experiments, 5 of the bladders required the use of the distributed model.  $R_p$  was increased significantly in acetate solutions, but was not affected by amiloride. The extraepithelial parameters  $R_x$  and  $R_s$  were increased significantly in

acetate solutions, however,  $C_x$  was unchanged. Amiloride did not significantly alter any of these parameters.

#### Discussion

The aim of this paper was two-fold. First, using impedance analysis and the known morphology of the toad urinary bladder, we develop an electrical equivalent circuit model for this epithelium. Second, we investigate the effect that altering transepithelial sodium transport has on the equivalent circuit parameters. The major findings are as follows:

(i) Impedance analysis shows that the toad urinary bladder must be modelled as an epithelial cell layer in series with an extraepithelial cell layer (see Fig. 1b). This model is substantiated by the known morphology of the toad bladder which consists of an epithelial cell layer plus a submucosa.

(ii) The ratio of the apical to basolateral membrane capacitance (a measure of surface area) is 1:4.6, suggesting that the basolateral membrane is some 5 times larger than the apical membrane surface area.

(iii) The magnitude of the resistance of the lateral intercellular space is inversely correlated with the degree of stretch applied to the epithelium, suggesting that stretch both dilates and shortens the lateral intercellular space.

(iv) The apical membrane contains an amiloride sensitive conductance in parallel with an amiloride insensitive conductance. This latter conductance accounts for approximately 10–20% of the total apical conductance.

(v) Inhibition of sodium transport by amiloride resulted in a decrease in both the apical and basolateral membrane conductance.

(vi) Solution anions have strong modulatory effects on both the apical and basolateral membrane conductances.

(vii) Apical and basolateral membrane capacitances did not change as a function of altered sodium trans-



port rate. Thus alterations in membrane conductance are not caused by large changes in membrane area, but are due to changes in specific membrane conductances.

#### *Significance of extra-epithelial circuit parameters*

Although the membrane parameters estimated using impedance analysis were essentially model-independent (see results), the data suggests the existence of a significant 'extra-epithelial barrier' in series with epithelial and the solution or series resistance.

Three morphological structures could account for the extraepithelial series RC required to fit toad bladder impedance data. The first candidate is the discontinuous layer of basal cells which are situated between the surface cells and basement membrane [13]. The second structure is the underlying layer of smooth muscle cell bundles and capillary beds. The third is the squamous epithelial cell layer which separates the muscle cells from the peritoneal cavity.

The following points suggest that the series RC is predominantly caused by the underlying muscle layer: (i) Impedance measurements performed on epithelial that have the smooth muscle layer removed (e.g., rabbit urinary bladder or descending colon) were adequately described by equivalent circuit models that did not include a series RC. (ii) If the basal cells or squamous epithelial layers were the source of the series RC, one would expect a direct correlation between apical membrane capacitance and  $C_x$ . Fig. 6A shows this is not the case;  $C_a$  and  $C_x$  are inversely correlated. This inverse correlation is consistent with the smooth muscle layer as the source of the series RC. In less stretched preparations,  $C_a$  is large and the smooth muscle bundles are packed on top of each other. An arrangement of the fibers in this manner will result in a low effective capacitance. In more stretched preparations, there is less overlap of the fibers, thereby increasing the effective capacitance. (iii) The magnitude of the resistor  $R_x$  should be directly proportional to apical membrane capacitance (i.e., stretch). As illustrated in Fig. 6B, this is the case. At higher values of  $C_a$  (less stretch) the resistance is higher. As  $C_a$  decreases (more stretch),  $R_x$  is decreased.  $R_x$  had a relatively low value ( $94 \Omega \text{ cm}^2$ ) and was unaffected by amiloride, although it was increased 60% and 90% in acetate and gluconate, respectively. This finding suggests that the resistance pathway is extracellular, i.e., between the cells. For these reasons, we tentatively conclude that the 'extracellular' RC is likely to be the subepithelial smooth muscle and connective tissue layers.

#### *Epithelial impedance properties*

(i) *Membrane capacitances and conductances.* Measurements of membrane capacitance allow one to accurately determine the rate of transport normalized to actual membrane area. The average apical membrane

capacitance for the toad bladder under normal conditions was  $\approx 0.9 \mu\text{F}/\text{cm}^2$ . Because of the predominance of granule cells in this epithelium, this value probably reflects primarily the membrane area of this cell type.

The ratio of 1:4.6 (apical to basolateral membrane capacitance) is similar to that reported for the rabbit urinary bladder of 1:4.8 [14], turtle urinary bladder of 1:2.5 [18], and *Necturus* gallbladder of 1:4.6 [19], and suggests that the basolateral membrane has approximately 5-times the surface area of the apical membrane. An unresolved question is the fraction of the apical membrane area and basolateral membrane area accounted for by each of the three different cell types.

In addition to measuring the average apical and basolateral membrane capacitances, impedance analysis also measures the average apical and basolateral membrane conductances. As shown in Fig. 3, there is a direct relationship between the amount of current flowing across the apical membrane and the apical membrane conductance. The basolateral membrane conductance measured from all bladders studied was  $1.6 \text{ mS}/\text{cm}^2$ , was not correlated with the cellular current ( $I_c$ ). In addition, the above basolateral membrane conductance is 5-times larger than that reported by Warncke and Lindemann (Refs. 20 and 21) using impedance analysis. Possible explanations for this discrepancy might be the composition of the Ringers (Warncke and Lindemann used a mucosal  $\text{NaSO}_4$  Ringers at pH 5.5) as well as the equivalent circuit model to estimate the membrane conductances (a simple lumped model was used). Estimates of the basolateral membrane conductance, using microelectrodes, range from low values of  $0.36\text{--}0.23 \text{ mS}/\text{cm}^2$  [22,23] to a high value of  $1.45 \text{ mS}/\text{cm}^2$  [24]. The latter value is in excellent agreement with the impedance estimates. Nagel and Van Driessche [24] suggest that previous estimates of basolateral membrane conductance might be artifactually low due to apical membrane damage caused by the microelectrode.

There are two additional explanations for why microelectrode and impedance estimates of the basolateral membrane conductance might differ. First, impedance analysis measures the total basolateral membrane conductance of all three cell types which comprise the bladder, whereas microelectrode techniques might only measure the conductance of the impaled cell type. Second, microelectrode studies assume a model in which the resistance of the lateral intercellular space and extra-epithelial structures are negligible, this assumption will result in an underestimate of the basolateral membrane conductance by approx. 22% [25].

(ii) *Lateral intercellular space resistance.* As shown in Fig. 5 there is a positive correlation between distributed lateral space resistance and the apical mem-

brane surface area, such that a less stretched preparation (large surface area) has a significant distributed resistance. Replacement of chloride with either gluconate or acetate increased  $R_p$  by approx. 70%. This increase is predicted since the resistivity of a sodium gluconate or sodium acetate Ringers is approx. 40% greater than the NaCl Ringers [26]. Of the preparations which demonstrated a significant distributed resistance, this value averaged  $104 \Omega \text{ cm}^2$ , similar to the value previously reported for the rabbit urinary bladder by Clausen et al. [14] of  $130 \Omega \text{ cm}^2$ . The above value for the toad bladder suggests that the lateral spaces are reasonably collapsed (in agreement with numerous micrographs, see, for example, Ref. 5) and seems not to be significantly affected by the rate of  $\text{Na}^+$  transport but rather by the degree of stretch which presumably decreases path length.

#### *Effects of amiloride on epithelial impedance*

As expected from previous studies [1], addition of amiloride to the mucosal bathing solutions resulted in a decrease in apical membrane conductance to a new lower value (see Table I and Fig. 3). This decrease occurred in the absence of a change in apical membrane area, in agreement with previous measurements on toad bladder [27,20] and rabbit urinary bladder [14]. The most straight-forward interpretation of this result is that amiloride directly inhibits the  $\text{Na}^+$  channel in agreement with fluctuation analysis studies [28].

Previous reports have shown that mucosal amiloride also causes a decrease in basolateral membrane conductance. In the present study this decrease was  $0.4 \text{ mS/cm}^2$ . This finding is in agreement with the micro-electrode results of Davis and Finn [22]. However, the decrease in conductance reported by these authors was 2 to 4-times less than the value reported above. Such a decrease can be caused by channel inactivation, modulation of the kinetics of a single channel or withdrawal of the channel in a membrane vesicle. If the latter mechanism involves a decrease in net membrane area, one would predict that the large basolateral conductance decrease would be correlated with a comparable decrease in membrane capacitance. As shown in Table II, the membrane capacitance did not change. This result suggests that the decrease in basolateral membrane conductance was not due to the net removal or endocytosis of a measurable quantity of basolateral membrane (and thus removal of conductive units). We must emphasize that this negative result does not exclude endocytosis as a possible down regulatory mechanism of membrane conductance. It simply implies that if such a mechanism exists the quantity of membrane removed is excessively small (i.e., perhaps the conductive units or channels are clustered).

An interesting finding was that the amiloride-sensitive  $\text{Na}^+$  transport increased with sequential addition

(for 10 min) and removal of a saturating dose of amiloride. This increase in transport was a result of a proportional increase in the amiloride sensitive apical membrane conductance, and not an increase in the net electrochemical gradient for  $\text{Na}^+$  entry. The amiloride-insensitive current and conductance were unaffected by amiloride as was the apical membrane capacitance. These latter observations again suggest that the increase in conductance is not a result of a simple increase in membrane area. Fig. 4 shows that after normalizing these currents to apical membrane area, the increase in current is independent of the initial current value, suggesting that mucosal amiloride is either directly or indirectly causing the activation of a quiescent population of  $\text{Na}^+$  channels. Similar increases in amiloride sensitive current can be elicited by preincubation of either the toad bladder [16] or frog skin [29] in  $\text{Na}^+$  free Ringers.

#### *Effect of anions on epithelial impedance*

We will first discuss the effects of anion replacement on the apical membrane impedance properties and then on the basolateral membrane properties.

(i) *Apical impedance.* Singer and Civan [4], were the first to report that mucosal replacement of  $\text{Cl}^-$  with different anions caused either a stimulation or inhibition of transepithelial  $\text{Na}^+$  transport. Similarly, Lewis et al. [5] found that symmetrical replacement of  $\text{Cl}^-$  with acetate caused a 25% increase in  $I_{sc}$  while replacement by gluconate led to a slower decrease in  $I_{sc}$  to a value which was 80% lower than in symmetrical  $\text{Cl}^-$  Ringers. This time-dependent decrease in  $I_{sc}$  to a new plateau value was directly related to the magnitude of the initial  $I_{sc}$ . Concomitant with the decrease in transport there was a decrease (on the average 66%) in cellular conductance. Lewis et al. [5] could not resolve whether the conductance decrease with gluconate occurred at the apical, basolateral, or both membranes. The present impedance measurements now reveal that gluconate causes a 50% decrease in both the apical and basolateral membrane conductances. Since the basolateral conductance is much larger than the apical conductance (in  $\text{Cl}^-$  Ringers it is 37-times larger), the predominant source of the transcellular conductance decrease caused by gluconate must occur at the apical membrane.

As mentioned previously, the apical membrane conductance is composed of amiloride sensitive and amiloride-insensitive components. Replacement of  $\text{Cl}^-$  by gluconate did not alter the conductance of the amiloride-insensitive component ( $9.5 \pm 1.3 \mu\text{S/cm}^2$  in  $\text{Cl}^-$  and  $7.5 \pm 1.2 \mu\text{S/cm}^2$  in gluconate  $n = 9$ ) but caused a large decrease ( $69 \pm 4\%$ ) in the amiloride sensitive conductance ( $35.3 \pm 5.5 \mu\text{S/cm}^2$  in  $\text{Cl}^-$  to  $10.6 \pm 2.2 \mu\text{S/cm}^2$  in gluconate  $n = 9$ ). The reversibility of this effect was assessed in 4 of the 9 studies. In these

experiments, the amiloride sensitive conductance was  $45.9 \pm 4.9 \mu\text{S}/\text{cm}^2$  in  $\text{Cl}^-$  Ringers, decreased to  $10.9 \pm 2.7 \mu\text{S}/\text{cm}^2$  in gluconate Ringers and recovered to  $23.8 \pm 2.0 \mu\text{S}/\text{cm}^2$  after replacing gluconate with  $\text{Cl}^-$  Ringers. Thus the amiloride-sensitive conductance only partially recovers after exposure to gluconate.

This partial recovery most probably reflects the effects of mucosal gluconate on the apical Na conductance. Lewis et al. [5] found that mucosal gluconate caused a rapid and reversible 40% inhibition of  $I_{\text{sc}}$ . In contrast, symmetrical gluconate solutions resulted in an irreversible 50% decrease in apical membrane amiloride sensitive Na permeability. Again, neither apical nor basolateral membrane permeability changes were associated with a net change in membrane area.

As mentioned above, replacement of  $\text{Cl}^-$  with acetate was previously reported to cause a 25% increase in transepithelial  $\text{Na}^+$  transport [5]. The site of this increase in transport was not determined. Using impedance analysis, we now report a significant ( $29 \pm 12\%$ ) increase in apical membrane amiloride-sensitive  $\text{Na}^+$  conductance. The reversibility of this stimulation was not tested in the present study. However, the increase in transport was not associated with an alteration in either apical or basolateral membrane capacitance. As in all other experiments, acetate did not alter the amiloride-insensitive apical membrane conductance.

(ii) *Basolateral impedance.* One of the major purposes of this paper was to determine whether the previously reported decrease in basolateral membrane  $\text{K}^+$  conductance caused by replacing  $\text{Cl}^-$  with gluconate (thus causing cell shrinkage) was due to: (1) the endocytosis of part of the basolateral membrane containing  $\text{K}^+$  channels or (2) inactivation of single channels or an alteration of their kinetics. Assuming that channels are equally distributed over the membrane, the first process will result in a decrease in both basolateral membrane area and conductance while the other mechanisms will show a decrease in conductance in the absence of an area change. As shown in Table III, basolateral capacitance did not change, although basolateral membrane conductance decreased by 50%. This suggests that simple withdrawal of large areas of membrane containing  $\text{K}^+$  channels is not the sole mechanism of  $\text{K}^+$  channel regulation at the basolateral membrane as such a withdrawal would decrease  $C_{\text{bl}}$ . As in the case of amiloride, we note that impedance studies cannot resolve the removal of small areas of densely clustered channels nor simultaneous withdrawal and replacement (i.e. coordinated endocytosis and exocytosis) of large membrane areas.

In contrast to gluconate, acetate replacement of  $\text{Cl}^-$  did not result in a change in basolateral membrane conductance nor capacitance. Lewis et al. [5] proposed that acetate was impermeable, but that the non-ionic

form of acetate could diffuse passively into the cell, loose its proton and thus become trapped [30]. These authors demonstrated that cells in acetate solutions did not shrink nor was basolateral membrane  $\text{K}^+$  conductance altered. If  $\text{K}^+$  permeability is linked to cell volume [5,31] then from the above points one would predict that  $\text{K}^+$  permeability would either remain constant or increase. The lack of change in basolateral conductance (Table IV) suggests that the  $\text{K}^+$  permeability might increase since replacement of  $\text{Cl}^-$  with the less permeant anion acetate should cause a decrease in basolateral conductance.

As shown for  $\text{Cl}^-$  Ringers, inhibition of  $\text{Na}^+$  transport using amiloride caused a large decrease in basolateral conductance in the presence of acetate Ringers but not a significant decrease in basolateral conductance when the epithelium was bathed in gluconate Ringers. The percent decrease in the basolateral membrane conductance is similar to the percent decrease in apical membrane  $\text{Na}^+$  conductance.

In conclusion, using impedance analysis, we have shown that the apical membrane of the toad urinary bladder contains two parallel conductances, one which is blocked by amiloride and one which is amiloride-insensitive. The apical membrane amiloride-sensitive conductance is greater after pre-incubation in amiloride and is not correlated with the initial amiloride-sensitive conductance, suggesting the recruitment of a separate quiescent pool of channels. Cell volume changes induced by symmetrical replacement of chloride by gluconate (to induce shrinkage) or acetate (to induce swelling) are accompanied by large changes in membrane conductances. Acetate increased the apical membrane amiloride-sensitive conductance whereas gluconate decreased both membrane conductances. All conductance changes occurred without alterations in the capacitance of either the apical or basolateral membranes. Consequently, the regulation of membrane conductances by these factors is not due to alterations in net membrane area.

## Acknowledgments

We gratefully acknowledge the technical assistance of W. Alles and J. Berg. This work was supported by NIH grants DK29962 to N.K.W., DK33243 and DK44321 to S.A.L., and an American Heart Association grant to C.C.

## References

- MacKnight, A.D.C., Dibona, D.R. and Leaf, A. (1980) *Physiol. Rev.* 60, 615–715.
- Diamond, J.M. (1982) *Nature* 300, 683–685.
- Schultz, S.G. (1981) *Am. J. Physiol.* 241, F579–F591.
- Singer, I. and Civan, M.M. (1971) *Am. J. Physiol.* 221, 1019–1026.
- Lewis, S.A., Butt, A.G., Bowler, M.T., Leader, J.P. and MacKnight, A.D.C. (1985) *J. Membr. Biol.* 83, 119–137.

- 6 Lewis, S.A. (1977) *Am. J. Physiol.* 232, F187-F295.
- 7 Yonath, J. and Civan, M.M. (1971) *J. Membr. Biol.* 5, 366.
- 8 Wills, N.K., Lewis, S.A. and Eaton, D.C. (1979) *J. Membr. Biol.* 45, 81-108.
- 9 Clausen, C., Reinach, P.S. and Marcus, D.C. (1986) *J. Membr. Biol.* 91, 213-225.
- 10 Valdiosera, R., Clausen, C. and Eisenberg, R.S. (1974) *J. Gen. Physiol.* 63, 432-459.
- 11 Wills, N.K. and Clausen, C. (1987) *J. Membr. Biol.* 95, 21-35.
- 12 Cole, K. (1972) *Membranes, Ions, and Impulses*, p. 12, University of California Press, Berkeley.
- 13 Choi, J.K. (1963) *J. Cell Biol.* 16, 53-72.
- 14 Clausen, C., Lewis, S.A. and Diamond, J.M. (1979) *Biophys. J.* 26, 291-318.
- 15 Hamilton, W.C. (1964) *Statistics in Physical Science*, pp. 69-88, Ronald Press, New York.
- 16 Garty, H. and Edelman, I.S. (1983) *J. Gen. Physiol.* 81, 785-803.
- 17 Sansom, S.C. and O'Neil, R.G. (1985) *Am. J. Physiol.* 248, F858-F868.
- 18 Clausen, C. and Dixon, T.E. (1984) *Curr. Top. Membr. Transp.* 20, 47-60.
- 19 Lim, J.J., Kottra, G., Kampmann, L. and Fromter, E. (1984) *Curr. Top. Membr. Transp.* 20, 27-46.
- 20 Warncke, J. and Lindemann, B. (1981) *Int. Cong. Physiol. Sci.* 28th Budapest, 1980, *Proceedings (Adv. Physiol. Sci. Vol. 3)*, 129-133.
- 21 Warncke, J. and Lindemann, B. (1985) *J. Membr. Biol.* 86, 255-265.
- 22 Davis, C.W. and Finn, A.L. (1982) *Science* 216, 525-527.
- 23 Reuss, L. and Finn, A.L. (1974) *J. Gen. Physiol.* 64, 1-25.
- 24 Nagel, W. and Van Driessche, W. (1989) *Pflügers. Arch.* 415, 121-123.
- 25 Boulpaep, E. and Sackin, H. (1980) *Curr. Top. Membr. Transp.* 13, 169-197.
- 26 Robinson, R.A. and Stokes, R.H. (1970) *Electrolyte solutions*, Butterworth, London, U.K.
- 27 Stetson, D.L., Lewis S.A., Alles, W. and Wade, J.B. (1982) *Biochim. Biophys. Acta* 689, 267-274.
- 28 Palmer, L.G., Li, J.H.Y., Lindemann, B. and Edelman, I.S. (1982) *J. Membr. Biol.* 64, 91-102.
- 29 Fisher, R.S., Baxendale, L.M. and Helman, S.I. (1986) *Fed. Proc.* 45, 516.
- 30 Cooke, K.R. and MacKnight, A.D.C. (1984) *J. Physiol. (London)* 349, 135-156.
- 31 Hudson, R.L. and Schultz, S.G. (1984) *Science* 224, 1237-1239.